Journal of Physiology (1991), **440**, *pp.* 131–142
With 6 figures
Printed in Great Britain

SODIUM- AND CALCIUM-DEPENDENT CONDUCTANCES OF NEURONES IN THE ZEBRA FINCH HYPERSTRIATUM VENTRALE PARS CAUDALE *IN VITRO*

BY M. KUBOTA AND N. SAITO

From the Department of Physiology, Dokkyo University School of Medicine, Mibu, Tochigi 321-02, Japan

(*Received 5 February 1990*)

SUMMARY

1. Intracellular recordings were made from zebra finch hyperstriatum ventrale pars caudale (HVc) neurones in *in vitro* slice preparations.

2. Small depolarizing current pulses elicited tonic firing while relatively large current pulses elicited an initial high-frequency burst followed by tonic firing. Time-dependent and fast-activated inward rectification were observed when a hyperpolarizing current pulse was applied.

3. Fast action potentials were abolished by tetrodotoxin (TTX, 0·5 μg/ml). When Co^{2+} (2·2–2·4 mM) was added to a low-Ca^{2+} (0–0·2 mM) solution, a plateau potential was elicited by a small depolarizing current pulse. These plateau potentials outlasted the applied current pulse and were abolished by TTX (0·5 μg/ml).

4. A long-lasting after-hyperpolarization (AHP), with a duration of tens of seconds, followed long trains of repetitive firing in control solution. Even in a low-Ca^{2+} (0–0·2 mM) solution containing Co^{2+} (2·2–2·4 mM) the long-lasting AHPs followed plateau potentials and were associated with an increase in input conductance. The long-lasting AHP, as well as the plateau potential, was blocked by TTX (0·5 μg/ml).

5. While TTX abolished fast action potentials, two types of active responses with different thresholds were elicited by depolarizing current in the presence of TTX (0·5 μg/ml), particularly when tetraethylammonium (5 mM) was also added to the solution. Both the low-threshold spike (LTS) and the high-threshold spike (HTS) were abolished by Co^{2+} (2·2–2·3 mM).

6. When Ba^{2+} (0·5–1 mM) was added to a solution containing TTX (0·5 μg/ml), an LTS elicited by a depolarizing current pulse became larger in amplitude. At membrane potentials more positive than −55 mV, an HTS, but not the LTS, was elicited.

7. These results suggest that HVc neurones have three Na^+-dependent conductances: a fast Na^+ conductance responsible for the fast spike, a persistent Na^+ conductance responsible for the plateau potential, and a Na^+-activated K^+ conductance responsible for the long-lasting AHP; and that they have two Ca^{2+}-dependent conductances: a low-threshold Ca^{2+} conductance responsible for the LTS, and a high-threshold Ca^{2+} conductance responsible for the HTS.

INTRODUCTION

Oscine birds like the zebra finch are characterized by their ability to sing complex songs. They have discrete, well-developed brain regions for song control, especially in males. This corresponds to behaviour in which normally only males sing. The nucleus hyperstriatum ventrale pars caudale (HVc) is one of the important nuclei in song control. The HVc is considered to be the premotor region for song production (Nottebohm, Stokes & Leonard, 1976; McCasland, 1987), and to be analogous to Broca's area in the human cerebral cortex.

Thus far, many anatomical and some physiological studies of song control nuclei, including the HVc, have been reported (e.g. Nottebohm, 1980; Konishi, 1985). However, no electrical membrane properties of the individual neurones in the HVc or any of the other song control nuclei have been studied. We describe here some electrical membrane properties and their underlying ionic conductances in zebra finch HVc neurones in brain slice preparations. Some of the present results have been presented in abstract form (Kubota & Saito, 1989).

METHODS

Slice preparation

Experiments were conducted on HVc neurones of adult male zebra finches (*Poephila quttata*). Animals were killed by rapid decapitation and the brain was rapidly removed and sectioned mid-sagittally. One hemisphere was cut frontally and its caudal half was cut sagittally. The medial two-thirds was then glued, medial side up, to a stage by cyanoacrylate and immersed in ice-cold oxygenated Krebs–Ringer solution. Sagittal 350 μm slices were prepared on a Microslicer (Dosaka EM, Japan). Slices were transferred to an interface-type incubation chamber perfused with Krebs–Ringer solution at 36 ± 1 °C. This solution consisted of (mM): NaCl, 124; KCl, 3; $MgSO_4$, 1·3; $CaCl_2$, 2·4; NaH_2PO_4, 1·24; $NaHCO_3$, 26; and glucose, 15; it was bubbled with 95% O_2/5% CO_2 and had a pH of 7·4. When $CoCl_2$ or $BaCl_2$ was added to the perfusing solution, $MgSO_4$ was replaced by $MgCl_2$, NaH_2PO_4 was omitted to avoid precipitation, and the corresponding $CaCl_2$ concentration was reduced to maintain the total concentration of divalent cations.

Intracellular recording

After incubating for at least 1·5 h, one slice at a time was placed in an interface-type recording chamber and perfused with Krebs–Ringer solution at 36 ± 1 °C. Intracellular recordings were made through glass microelectrodes filled with 3 M-potassium acetate (titrated to pH 7·2 with acetic acid). The DC resistance of the electrodes was 40–100 MΩ. Under a binocular light microscope, the HVc could be clearly recognized in the slice. A conventional amplifier with an active bridge circuit was used for passing current through the recording microelectrode. Data were stored on tape using an FM data recorder (R-510, TEAC, Japan) or videotape using a pulse-code modulation data processor (PCM-501 ES, Sony, Japan).

In some experiments horseradish peroxidase (HRP) was injected into neurones by depolarizing current pulses (0·8–1·2 nA, 0·7 s, 1 Hz) for 8–25 min. HRP (4–6%) was dissolved in 1 M-potassium acetate and 0·05 M-Tris buffer (pH 7·6). After fixing with 4% glutaraldehyde in 0·1 M-phosphate buffer (pH 7·4) for 2 h at 4 °C, slices were immersed in 30% sucrose in 0·1 M-phosphate buffer (pH 7·4) overnight at 4 °C. Sections 60 μm thick were cut on a freezing microtome. HRP was visualized by the method of Hanker–Yates (Hanker, Yates, Metz & Rustioni, 1977).

Tetrodotoxin (TTX) was obtained from Sigma (USA). Tetraethylammonium (TEA) was obtained from Wako (Japan). Hanker–Yates reagent was obtained from Polysciences (USA). HRP was obtained from Toyobo (Japan).

RESULTS

The results reported here are based on recordings from 101 neurones with a resting membrane potential exceeding −55 mV, and an overshooting action potential. The mean resting potential of the HVc neurones was −63±4·7 mV (mean±S.D., n =

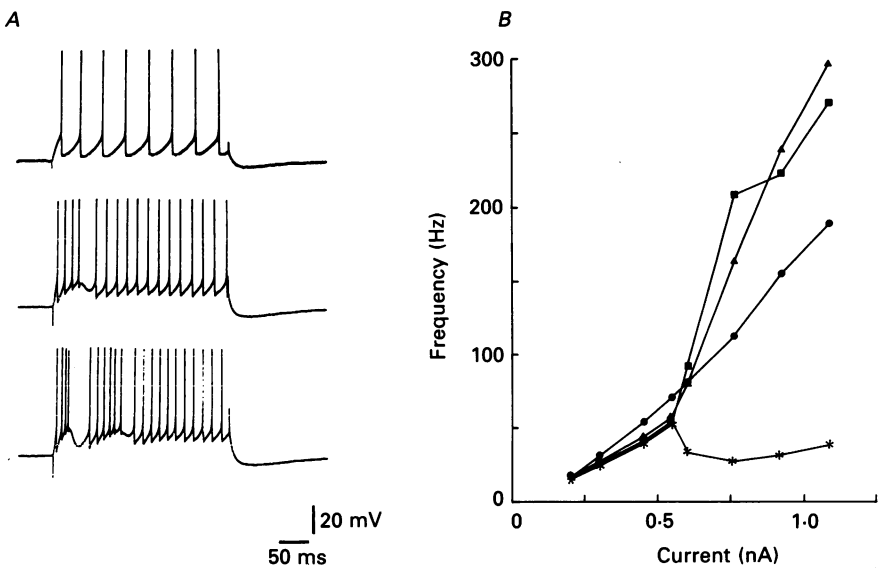

Fig. 1. Firing properties. *A*, voltage responses to depolarizing current pulses. A small depolarizing current pulse (0·3 nA) elicited tonic firing (top). A large depolarizing current pulse (0·6 nA) elicited an initial high-frequency burst followed by tonic firing (middle). A larger depolarizing current pulse (0·76 nA) elicited two trains of burst firing (bottom). *B*, plots of the frequency–current relation for the first four interspike intervals for the cell shown in *A*. Circles represent the first interspike interval, triangles the second, squares the third, and asterisks the fourth. Resting membrane potential was −64 mV.

101), the action potential amplitude 73±6·4 mV (n = 101) and the input resistance 93±33 MΩ (n = 99). Input resistances were determined by responses to small hyperpolarizing current pulses (0·1–0·2 nA, 300 ms).

Firing properties

Tonic firing was elicited by small depolarizing current pulses (Fig. 1*A*). When the current increased to a certain level, however, the firing frequency for the first several spikes increased to produce an initial short burst followed by tonic firing and more intense current sometimes elicited trains of bursts (Fig. 1*A*). The plots of the interspike interval frequency *versus* applied current for this cell show that the transition from tonic firing to high-frequency burst occurred at a current of 0·6 nA and the fourth interval frequency exhibited a negative slope region corresponding to the transition (Fig. 1*B*). Burst firing followed by tonic firing was observed in most of the HVc neurones examined (seventy-seven of eighty-six cells). Burst firing was never elicited by current less intense than that required to elicit the tonic firing.

Inward rectification

Hyperpolarizing current pulses elicited voltage responses which exhibited voltage-dependent inward rectification (Fig. 2*A*). The plots of the voltage response *versus* applied current show that time-dependent inward rectification was elicited at

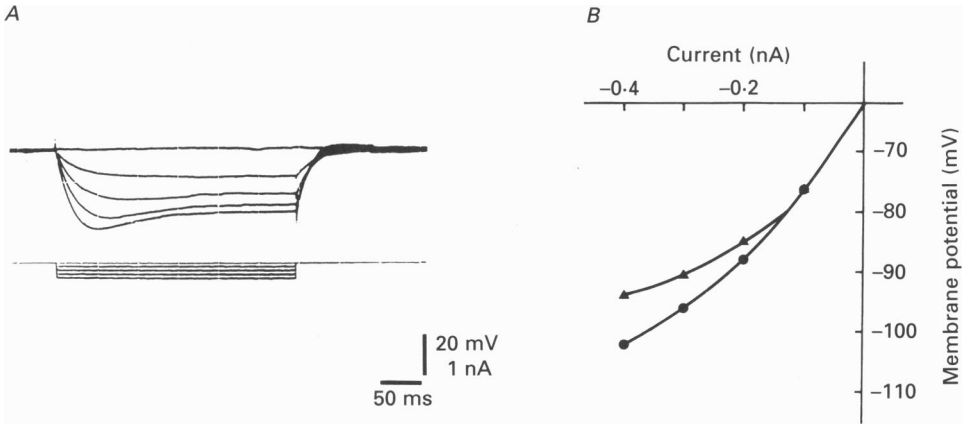

Fig. 2. Inward rectification. *A*, superimposed voltage responses to hyperpolarizing current pulses. *B*, plots of the voltage response *versus* applied current shown in *A*. Circles represent the peak voltage responses and triangles the voltage responses at the end of the current pulses. Upper traces, voltage records; lower traces, applied currents in this and subsequent figures. Resting membrane potential was −62 mV.

membrane potentials more negative than −80 mV (Fig. 2*B*). The peak voltage responses also exhibited inward rectification over the same range of membrane potentials as the time-dependent inward rectification (Fig. 2*B*). Thus two kinds of inward rectification, time-dependent and fast-activated, seemed to be present in the HVc neurones. Most of the HVc neurones exhibited both the time-dependent and the fast-activated inward rectification (eighty-one of ninety-nine cells).

Plateau potential

To examine conductances underlying the firing properties, we first blocked Ca^{2+} influx by reducing the extracellular Ca^{2+} concentration (0–0·2 mM) and adding Co^{2+} (2·2–2·4 mM) to the perfusing solution. Figure 3 shows that in the presence of Co^{2+}, the after-hyperpolarization (AHP) following the fast action potential decreased in amplitude and, even during small depolarizing current pulses, a slowly rising plateau potential developed during the first 100 ms; the fast action potentials on the rising phase of the plateau progressively decreased in amplitude becoming totally inactivated at the peak of the plateau. The plateau potential often outlasted the applied current pulse and it was always followed by a long-lasting AHP (Fig. 3*C*). The timing of the appearance of the plateau potential paralleled that of the reduction in the spike AHP. The plateau potential could be elicited by current pulses as short as 5 ms. Both the fast spikes and the plateau potential were blocked by TTX (0·5 μg/ml, Fig. 3*D*). The blockage by TTX of the plateau potential which appeared in the presence of Co^{2+} suggests that the plateau potential is produced by a persistent or slowly inactivating Na^+ conductance.

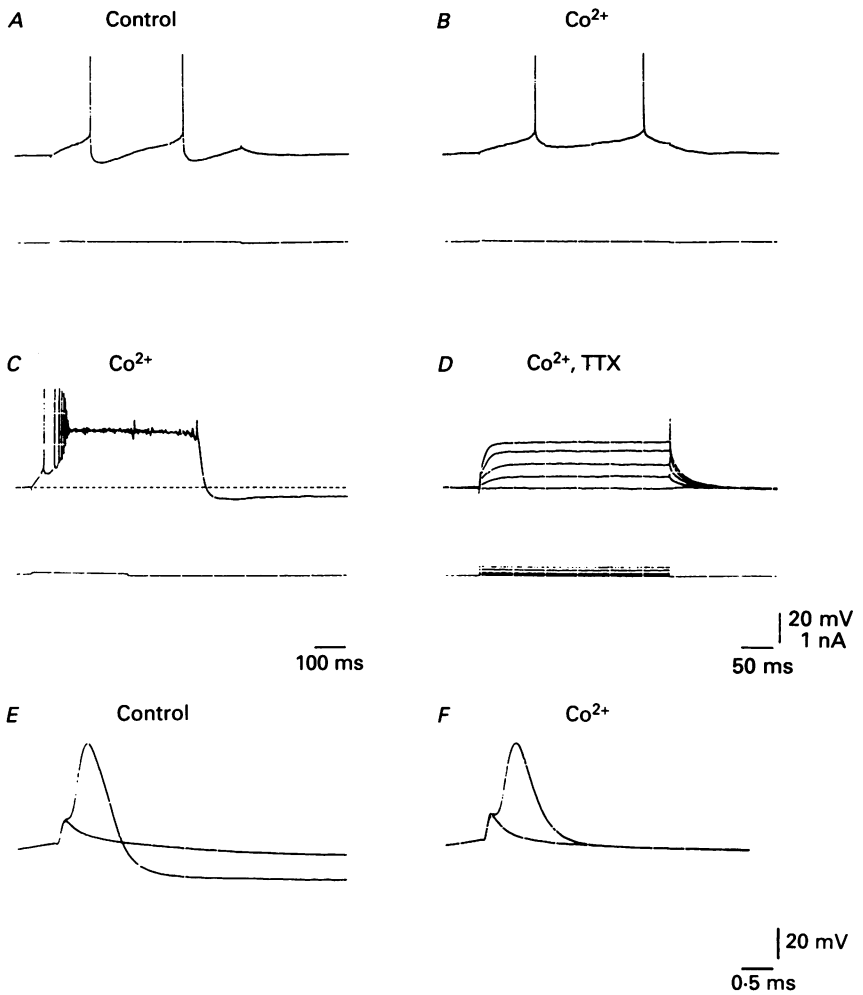

Fig. 3. Plateau potential. *A*, voltage response to a depolarizing current pulse in control solution. *B*, voltage response to a depolarizing current pulse slightly less intense than that shown in *A* (by 0·01 nA) in low-Ca^{2+} (0·1 mM) solution containing Co^{2+} (2·3 mM). *C*, plateau potential elicited by a depolarizing current pulse in low-Ca^{2+} solution containing Co^{2+}. The plateau potential outlasted the applied current. Note hyperpolarization after the plateau potential. *D*, superimposed voltage responses to depolarizing current pulses after addition of TTX (0·5 μg/ml) to the low-Ca^{2+} solution containing Co^{2+}. TTX blocked both the fast spikes and the plateau potential. Note also the absence of the hyperpolarization seen in *C*. *E* and *F*, action potentials elicited by brief (3 ms) current pulses shown at fast sweep. *E*, action potential in control solution. *F*, action potential in Ca^{2+}-free solution containing Co^{2+} (2·4 mM). Each action potential is superimposed on a just-subthreshold response. *A–D* are from the same cell. Resting membrane potential was −59 mV. *E* and *F* are from another cell. Resting membrane potential was −66 mV.

The reduction by Co^{2+} of the AHP following the fast action potential (Fig. 3*B* and *F*) suggests that this AHP is produced by a Ca^{2+}-activated K^+ conductance. However, a different conductance must underlie the long-lasting hyperpolarization which follows the plateau potential in the Co^{2+}-containing solution (Fig. 3*C*). This AHP is described next.

Long-lasting after-hyperpolarization

After sufficient repetitive firing was elicited, a long-lasting AHP with a duration of tens of seconds was observed in control solution in all HVc neurones examined ($n = 28$). Firing frequency higher than 30 Hz elicited by currents of 0·4–1·25 nA with

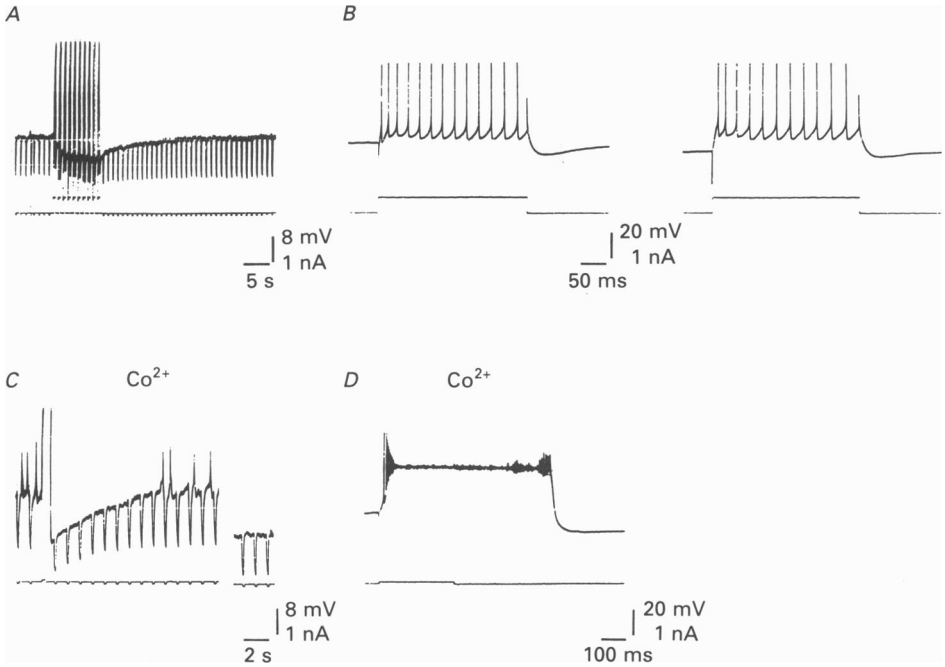

Fig. 4. Long-lasting after-hyperpolarization (AHP). *A*, long-lasting AHP elicited by ten depolarizing current pulses (300 ms) at 1 Hz in control solution. Hyperpolarizing current pulses (150 ms) were applied to monitor the input conductance change during the AHP. The input conductance increased during the long-lasting AHP. *B*, voltage response to the first depolarizing current pulse (left) and that to the tenth current pulse (right) which elicited the long-lasting AHP in *A*. Thirteen spikes in the first response reduced to eleven spikes in the tenth response. *C*, long-lasting AHP in Ca^{2+}-free solution containing Co^{2+} (2·4 mM). Note the increase in input conductance during the long-lasting AHP, even when compared to that at similarly hyperpolarized membrane potential induced by DC current injection. *D*, plateau potential which elicited long-lasting AHP in *C*. *A–D* are from the same cell. Resting membrane potential was −60 mV.

300 ms duration was required for this long-lasting AHP to develop. Figure 4*A* shows that during ten pulses, each of which elicited repetitive firing followed by a long-lasting AHP, the long-lasting AHP summated; when stimulation stopped this summed response decayed over tens of seconds. The input conductance increased and the cell excitability (indicated by firing frequency) was reduced during the long-lasting AHP (Fig. 4*A* and *B*). When Co^{2+} (2·4 mM) was added to a Ca^{2+}-free perfusing solution, the long-lasting AHP remained unchanged and was generated after the plateau potential (Fig. 4*C* and *D*). During the long-lasting AHP the input conductance increased, even when compared to that at a similarly hyperpolarized

membrane potential (Fig. 4*C*). This long-lasting AHP, as well as the plateau potential, was blocked by TTX as described above (see Fig. 3*D*). These results suggest that the long-lasting AHP may be a Na^+-dependent but not a Ca^{2+}-dependent potential.

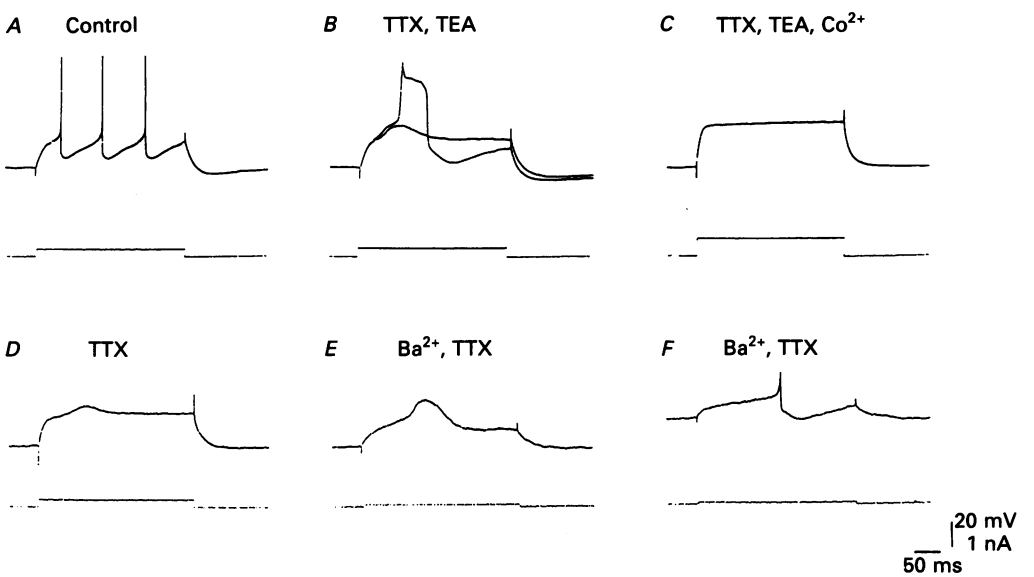

Fig. 5. Low-threshold spike (LTS) and high-threshold spike (HTS). The cell was hyperpolarized to −74 mV by DC current injection in *A–C*. Resting membrane potential was −60 mV. *A*, voltage response to a depolarizing current pulse in control solution. The rate of rise of the action potential was 386 V/s. *B*, LTS and HTS in solution containing TTX (0·5 μg/ml) and TEA (5 mM). The rate of rise of the HTS was 41 V/s. *C*, both the LTS and the HTS were blocked in low-Ca^{2+} (0·1 mM) solution containing Co^{2+} (2·3 mM), TTX and TEA. *D*, LTS in solution containing TTX (0·5 μg/ml) from another cell. The cell was hyperpolarized to −71 mV by DC current injection in *D* and *E*. *E*, LTS after Ba^{2+} (1 mM) was added to the solution containing TTX and Ca^{2+} (1·4 mM). *F*, HTS at a depolarized membrane potential (−50 mV) in the presence of Ba^{2+} (1 mM), Ca^{2+} (1·4 mM) and TTX. Resting membrane potential was −56 mV.

TTX-sensitive action potential

In control solution, action potentials with fast time course (0·48 ± 0·08 ms duration at one-half amplitude, $n = 24$) were elicited by depolarizing current pulses (Fig. 3*E*). These action potentials were abolished by TTX but not by Co^{2+} (Fig. 3*D* and *F*). Addition of Co^{2+} and reduction of Ca^{2+} slowed the last half of the falling phase of the fast action potential and blocked the AHP following the fast action potential (Fig. 3*F*).

TTX-insensitive action potentials

While fast action potentials could not be elicited in the presence of TTX (Fig. 3*D*), two types of prolonged active responses with different thresholds were elicited by depolarizing current in the presence of TTX (0·5 μg/ml); a high-threshold response was elicited particularly when TEA (5 mM) was also added to the TTX-containing

solution to reduce K^+ conductances (Fig. 5*A–C*). When the current intensity was low, only a small, low-threshold spike (LTS) was elicited. A large, high-threshold spike (HTS) was also elicited by slightly more intense current (Fig. 5*B*). The HTS had a distinct inflexion on the rising phase corresponding to the LTS. Both the LTS

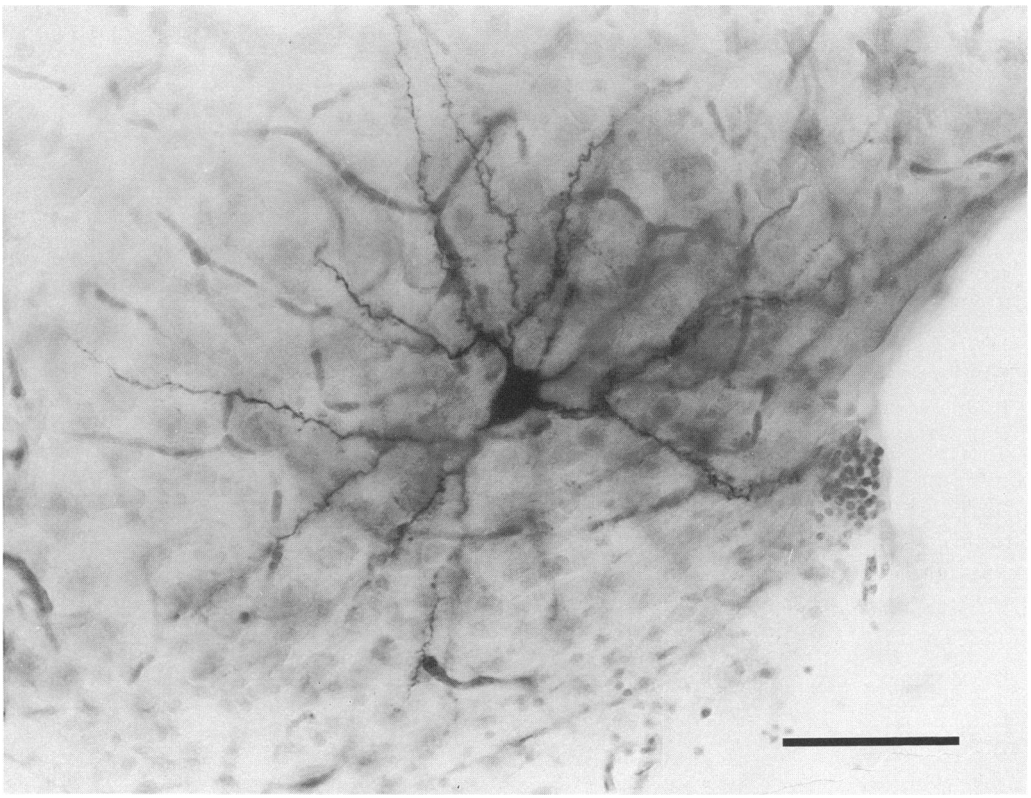

Fig. 6. HVc neurone stained by intracellular injection of HRP. Counter-stained with cresyl violet. Scale bar, 50 μm.

and the HTS were abolished when Co^{2+} (2·2–2·3 mM) was added to the low-Ca^{2+} (0·1–0·2 mM) solution (Fig. 5*C*). These results suggest that the LTS and the HTS co-exist in the HVc neurones and that both are Ca^{2+}-dependent responses.

Low- and high-threshold spikes in the presence of Ba^{2+} and TTX

To further ascertain the co-existence of the LTS and the HTS, Ba^{2+} (0·5–1 mM) was added to a perfusing solution containing TTX (0·5 μg/ml) and reduced Ca^{2+} (1·4–1·9 mM) because Ba^{2+} is known to flow through Ca^{2+} channels better than Ca^{2+} and to block some kinds of K^+ channels (Hagiwara, Fukuda & Eaton, 1974; Schwindt & Crill, 1980). When a cell was hyperpolarized from the resting membrane potential to prevent inactivation of the LTS, a small LTS was elicited by a depolarizing current pulse in TTX-containing solution (Fig. 5*D*). The LTS became larger in amplitude followed by a small AHP when Ba^{2+} (1 mM) was added to the

solution containing TTX and Ca^{2+} (1·4 mM; Fig. 5*E*). When a cell was depolarized to a potential more positive than −55 mV, no LTS was elicited, but an HTS was elicited by a depolarizing current pulse (Fig. 5*F*). The LTS seen at hyperpolarized potentials seemed to be inactivated by depolarization of the membrane to a potential more positive than −55 mV. The smaller amplitude and shorter duration of the HTS in the presence of Ba^{2+} and TTX than that in the presence of TEA and TTX may be due to a partial substitution of Ca^{2+} with Ba^{2+}. A fast Ca^{2+}-activated K^+ conductance which may be highly sensitive to TEA (Adams, Constanti, Brown & Clark, 1982) will be activated by residual Ca^{2+} and reduce the amplitude and duration of the HTS.

Morphological features

In four experiments, HRP was injected intracellularly to examine the morphological features of neurones that had the characteristic properties described above. Figure 6 shows one of these cells. The soma size was relatively large ($15·3 \pm 0·84$ μm, mean soma diameter, $n = 4$) for HVc neurones. Each neurone had a relatively large dendritic field and multipolar dendrites with many spines.

DISCUSSION

The present study provides information about electrical activity and the underlying ionic conductances in zebra finch HVc neurones, which are important in song control. The HVc neurones reported here were characterized by a long-lasting AHP and high-threshold burst firing. These properties appeared to be related to, respectively, Na^+-dependent and Ca^{2+}-dependent conductances.

Na^+-dependent conductances

Fast action potential and plateau potential

Although Co^{2+} slowed the last half of the falling phase of the fast action potential, suggesting the presence of a fast Ca^{2+}-activated K^+ conductance in the falling phase of the fast action potential (Storm, 1987), Co^{2+} did not block the main part of the fast action potential. It was blocked by TTX. Thus, it seems likely that the main part of the fast action potential was produced by a voltage-dependent Na^+ conductance (Hodgkin & Huxley, 1952).

In addition to the fast action potential, HVc neurones have a TTX-sensitive plateau potential. This plateau potential was most evident in a low-Ca^{2+} solution containing Co^{2+}. Since the plateau potential was blocked by TTX but not by Co^{2+}, and it persisted during or outlasted the applied current, it was probably produced by a persistent or slowly inactivating Na^+ conductance. A persistent or slowly inactivating Na^+ conductance has been shown to be present in various vertebrate neurones (Llinás & Sugimori, 1980; Connors, Gutnick & Prince, 1982; Stafstrom, Schwindt & Crill, 1982; Jahnsen & Llinás, 1984; Jahnsen, 1986; Hirsch & Oertel, 1988; Yoshimura & Jessell, 1989). Since the plateau potential continues to be activated beyond the firing threshold of the fast spike, it is likely that this conductance is important in maintaining the tonic firing seen in HVc neurones.

Long-lasting after-hyperpolarization

Long-lasting AHPs (tens of seconds in duration) accompanied by an increase in input conductance were elicited after sufficient repetitive firing in control solution. A similar long-lasting AHP was generated after the plateau potential was elicited in Ca^{2+}-free solution containing Co^{2+}. When TTX was added to the perfusing solution, both this long-lasting AHP and the plateau potential were abolished. Although it is possible that the long-lasting AHP seen in control solution may be produced by a Ca^{2+}-activated K^+ conductance, the long-lasting AHP seen in Ca^{2+}-free solution cannot be Ca^{2+} dependent. This long-lasting AHP may be produced by a slow Na^+-activated K^+ conductance similar to that reported in mammalian neocortex neurones (Schwindt, Spain, Foehring, Chubb & Crill, 1988; Schwindt, Spain & Crill, 1989). This may differ from the fast Na^+-activated K^+ conductance which is assumed to be responsible for the repolarization of the fast action potential shown in some neurones of vertebrates (Bader, Bernheim & Bertrand, 1985; Dryer, Fujii & Martin, 1989) and invertebrates (Hartung, 1985).

Ca^{2+}-dependent conductances

The low- and high-threshold spikes

In the present study two types of TTX-insensitive spikes were observed: LTS and HTS. These co-existed in HVc neurones and both were blocked by Co^{2+}. Both were also elicited more readily when Ba^{2+} was added to perfusing solution containing TTX. Therefore, it is likely that the LTS and the HTS are produced by voltage-dependent Ca^{2+} conductances. Since the LTS was inactivated by membrane depolarization while the HTS remained activated, the LTS and the HTS may be produced by different kinds of Ca^{2+} conductances, low-threshold and high-threshold, respectively. As the LTS is inactivated at membrane potentials more positive than -55 mV, it may be similar to that seen in other neurones (Llinás & Yarom, 1981; Jahnsen & Llinás, 1984).

Burst firing

Burst firing was elicited by a relatively large depolarizing current pulse in HVc neurones. However, unlike bursting in other neurones such as thalamic neurones, this burst firing never occurred before tonic firing even when the membrane was hyperpolarized to levels more negative than the resting potential. Thus the burst firing of the HVc neurones is classified as a high-threshold type (Gerber, Greene & McCarley, 1989).

In HVc neurones the LTS alone seems to be insufficient to generate burst firing for the following reasons: first, the current required to elicit burst firing was much larger than that required for tonic firing, even when depolarizing current was applied to a hyperpolarized membrane from which the LTS could be fully activated; second, sometimes two or three trains of burst firing were elicited by one depolarizing current pulse (see Fig. 1*A*) during which the membrane potential was depolarized such that the LTS was inactivated. The burst firing of the HVc neurones, therefore, may require an additional depolarization by the HTS following the LTS.

Identification of neurones

The HVc projects to two other song-control regions: area X of the lobus parolfactorius and the nucleus robustus archistriatalis (RA) (Nottebohm, Kelley & Paton, 1982; Bottjer, Halsema, Brown & Miesner, 1989). Katz & Gurney (1981) showed that, in zebra finches, HVc neurones that had auditory responses projected to area X, and RA-projecting cells did not show auditory responses. They also showed that the area X-projecting cells had larger soma diameters and dendritic fields than the RA-projecting cells. Although we lack direct evidence about the projection areas of the HVc neurones recorded from in this study, it seems likely that they are the area X-projecting cells, because their morphological features are those of area X-projecting cells, i.e. relatively large soma size, large dendritic fields and many spines on the dendrites. The HVc neurones stained in this study also correspond to the type of thick dendrite cell classified in Golgi-impregnated HVc neurones of the canary (Nixdorf, Davis & DeVoogd, 1989).

We thank Dr H. Sakaguchi for help in preparing the slices and Mr H. Kaneko and Ms R. Kawakubo for help in preparing the illustrations. We also thank Dr A. Simpson for reading the manuscript. This work was supported in part by Grant-in-Aid for Scientific Research (63770093) from the Japanese Ministry of Education, Science and Culture.

REFERENCES

ADAMS, P. R., CONSTANTI, A., BROWN, D. A. & CLARK, R. B. (1982). Intracellular Ca^{2+} activates a fast voltage-sensitive K^+ current in vertebrate sympathetic neurones. *Nature* **296**, 746–749.

BADER, C. R., BERNHEIM, L. & BERTRAND, D. (1985). Sodium-activated potassium current in cultured avian neurones. *Nature* **317**, 540–542.

BOTTJER, S. W., HALSEMA, K. A., BROWN, S. A. & MIESNER, E. A. (1989). Axonal connections of a forebrain nucleus involved with vocal learning in zebra finches. *Journal of Comparative Neurology* **279**, 312–326.

CONNORS, B. W., GUTNICK, M. J. & PRINCE, D. A. (1982). Electrophysiological properties of neocortical neurons *in vitro*. *Journal of Neurophysiology* **48**, 1302–1320.

DRYER, S. E., FUJII, J. T. & MARTIN, A. R. (1989). A Na^+-activated K^+ current in cultured brain stem neurones from chicks. *Journal of Physiology* **410**, 283–296.

GERBER, U., GREENE, R. W. & MCCARLEY, R. W. (1989). Repetitive firing properties of medial pontine reticular formation neurones of the rat recorded *in vitro*. *Journal of Physiology* **410**, 533–560.

HAGIWARA, S., FUKUDA, J. & EATON, D. S. (1974). Membrane current carried by Ca, Sr and Ba in barnacle muscle fibers during voltage-clamp. *Journal of General Physiology* **63**, 564–578.

HANKER, J. S., YATES, P. E., METZ, C. B. & RUSTIONI, A. (1977). A new specific, sensitive and non-carcinogenic reagent for the demonstration of horseradish peroxidase. *Histochemical Journal* **9**, 789–792.

HARTUNG, K. (1985). Potentiation of a transient outward current by Na^+ influx in crayfish neurones. *Pflügers Archiv* **404**, 41–44.

HIRSH, J. A. & OERTEL, D. (1988). Intrinsic properties of neurones in the dorsal cochlear nucleus of mice, *in vitro*. *Journal of Physiology* **396**, 535–548.

HODGKIN, A. L. & HUXLEY, A. F. (1952). A quantitative description of membrane current and its application to conduction and excitation in nerve. *Journal of Physiology* **117**, 500–544.

JAHNSEN, H. (1986). Extracellular activation and membrane conductances of neurones in the guinea-pig deep cerebellar nuclei *in vitro*. *Journal of Physiology* **372**, 149–168.

JAHNSEN, H. & LLINÁS, R. (1984). Ionic basis for the electroresponsiveness and oscillatory properties of guinea-pig thalamic neurones *in vitro*. *Journal of Physiology* **349**, 227–247.

KATZ, L. C. & GURNEY, M. E. (1981). Auditory responses in the zebra finch's motor system for song. *Brain Research* **211**, 192–197.

KONISHI, M. (1985). Birdsong: from behavior to neuron. *Annual Review of Neuroscience* **8**, 125–170.

KUBOTA, M. & SAITO, N. (1989). Electrical membrane properties of zebra finch song control nucleus neurons *in vitro*. *Neuroscience Research Supplement* **9**, S76.

LLINÁS, R. & SUGIMORI, M. (1980). Electrophysiological properties of *in vitro* Purkinje cell somata in mammalian cerebellar slices. *Journal of Physiology* **305**, 171–195.

LLINÁS, R. & YAROM, Y. (1981). Properties and distribution of ionic conductances generating electroresponsiveness of mammalian inferior olivary neurones *in vitro*. *Journal of Physiology* **315**, 569–584.

MCCASLAND, J. S. (1987). Neuronal control of bird song production. *Journal of Neuroscience* **7**, 23–39.

NIXDORF, B. E., DAVIS, S. S. & DEVOOGD, T. J. (1989). Morphology of Golgi-impregnated neurons in hyperstriatum ventralis, pars caudalis in adult male and female canaries. *Journal of Comparative Neurology* **284**, 337–349.

NOTTEBOHM, F. (1980). Brain pathways for vocal learning in birds: a review of the first ten years. *Progress in Psychobiology and Physiological Psychology* **9**, 85–124.

NOTTEBOHM, F., KELLEY, D. B. & PATON, J. A. (1982). Connections of vocal control nuclei in the canary telencephalon. *Journal of Comparative Neurology* **207**, 344–357.

NOTTEBOHM, F., STOKES, T. M. & LEONARD, C. M. (1976). Central control of song in the canary, *Serinus canarius*. *Journal of Comparative Neurology* **165**, 457–486.

SCHWINDT, P. C. & CRILL, W. E. (1980). Effects of barium on cat spinal motoneurons studied by voltage clamp. *Journal of Neurophysiology* **44**, 827–846.

SCHWINDT, P. C., SPAIN, W. J. & CRILL, W. E. (1989). Long-lasting reduction of excitability by a sodium-dependent potassium current in cat neocortical neurons. *Journal of Neurophysiology* **61**, 233–244.

SCHWINDT, P. C., SPAIN, W. J., FOEHRING, R. C., CHUBB, M. C. & CRILL, W. E. (1988). Slow conductances in neurons from cat sensorimotor cortex *in vitro* and their role in slow excitability changes. *Journal of Neurophysiology* **59**, 450–467.

STAFSTROM, C. E., SCHWINDT, R. C. & CRILL, W. E. (1982). Negative slope conductance due to a persistent subthreshold sodium current in cat neocortical neurons *in vitro*. *Brain Research* **236**, 221–226.

STORM, J. F. (1987). Action potential repolarization and a fast after-hyperpolarization in rat hippocampal pyramidal cells. *Journal of Physiology* **385**, 733–759.

YOSHIMURA, M. & JESSELL, T. M. (1989). Primary afferent-evoked synaptic responses and slow potential generation in rat substantia gelatinosa neurons *in vitro*. *Journal of Neurophysiology* **62**, 96–108.